NJC

PAPER

Impact of chirality on the aggregation modes of L-phenylalanine- and D-glucose-decorated phenylene–thiophene oligomers†

Omar Hassan Omar,*[a] Marta Falcone,‡[b] Alessandra Operamolla[b] and Gianluigi Albano§*[b]

Cite this: DOI: 10.1039/d1nj02125g

Received 30th April 2021,
Accepted 31st May 2021

DOI: 10.1039/d1nj02125g

rsc.li/njc

The aggregation modes of three L-phenylalanine- or D-glucose-functionalized phenylene–thiophene oligomers were investigated using UV-Vis absorption and electronic circular dichroism (ECD) spectroscopies in both solution aggregation and thin film states. The ECD measurements revealed superior capability to provide information about their first level of supramolecular organization and to detect the possible co-existence of multiple aggregation pathways, very difficult to identify by using only UV-Vis absorption. The impact on the (chiro)optical response of the nature of the chiral pendant group, especially in terms of intermolecular hydrogen bonding and steric hindrance, as well as that of the oligothiophene π-conjugated length, will be elucidated. The ability to recognize and control different aggregation modes could be very useful for the preparation of thin films of π-conjugated oligomers with highly tunable chiroptical features in view of optical sensing and other innovative opto-electronic applications.

Introduction

Organic π-conjugated materials play a prominent role in optoelectronic and nanotechnology applications, such as an active layer[1,2] in organic light-emitting diodes (OLEDs),[3,4] organic photovoltaic (OPV) cells,[5] organic field-effect transistors (OFETs)[6] and sensors.[7] The intrinsic properties of organic π-conjugated systems (such as light absorption, emission, related energy gap, *etc.*) can be finely modulated for the desired application not only by chemical structure modifications, but also by controlling their organization in the solid state at different levels of hierarchy, from the first-order supramolecular arrangement[8–10] to the nano/mesoscale.[11,12] A crucial aspect is the possibility of different local domains; the same molecular system may undergo competing aggregation pathways during film fabrication, leading to polymorphic aggregated phases (kinetic *vs.* thermodynamic states), each featuring different optoelectronic properties.[13,14] The ability to recognize and control these different aggregation modes, especially in the case of thin films, would be useful for obtaining layers of chiral π-conjugated systems with highly tunable properties for innovative optoelectronic applications.[15]

Chirality also is a further valuable tool for controlling the structural organization of π-conjugated molecules at all hierarchical levels;[15] stereodefinite chiral elements in the molecular structure can drive their self-organization towards chiral supramolecular architectures, such as self-assembled helices, spirals or chiral sheets;[16–19] this first-order supramolecular chirality could be transferred to larger scale chiral morphologies, generating twisted ribbons, helical fibers and other supramolecular aggregation patterns.[17,20] Chiral functionalities tend to favour regularly twisted π-stacked arrangements, affecting in a reproducible way the fundamental electro-optical properties such as exciton migration and light emission, which in some cases may be hampered by too intense co-facial interactions.[16,21] In this regard, the introduction of chiral appendages in π-conjugated systems as organic semiconductors in photonics and electronics opens the way to highly innovative technological applications such as transistors based on enantioselective sensing layers for chiral analytes in the vapour phase,[22] enantiopure chiral magnets,[23] chirality-induced spin selectivity (CISS),[24] enantioselective electrochemical sensors,[25] detection/production of circularly polarized (CP) light.[26] In these devices, the active layers made of a chiral π-

[a] CNR-ICCOM Istituto di Chimica dei Composti Organometallici, Via Edoardo Orabona 4, Bari 70126, Italy. E-mail: hassan@ba.iccom.cnr.it
[b] Dipartimento di Chimica e Chimica Industriale, Università di Pisa, Via Giuseppe Moruzzi 13, Pisa 56124, Italy

† Electronic supplementary information (ESI) available: Experimental details and supplementary figures. See DOI: 10.1039/d1nj02125g

‡ Present address: Valsynthese SA, Fabrikstrasse 48, CH-3900 Brig, Switzerland.
§ Present address: Dipartimento di Chimica, Università degli Studi di Bari "Aldo Moro", *Via* Edoardo Orabona 4, 70126 Bari, Italy. E-mail: gianluigi.albano@uniba.it

conjugated system (in particular small molecules) as neat materials are still relatively uncommon, although this represents a clear advantage in terms of simplicity, reproducibility and ease of preparation.

Instrumental techniques able to characterize aggregation states at multiple hierarchical levels are fundamental for clarifying the structure–property relationships of such systems.[11,12,27] Chiroptical spectroscopies, and in particular electronic circular dichroism (ECD), play a central role in the elucidation of the aggregation pattern of chiral π-conjugated systems, providing valuable information about the first level of supramolecular organization at the nanometre scale for both solution and solid states, often complementary to that provided by microscopy techniques.[28–31]

Thiophene-based polymers represent one of the most interesting families of conductive polymers for optoelectronic applications.[32,33] It is not surprising that chiral oligo- and poly-thiophene derivatives are frequently investigated by ECD spectroscopy. An interesting motif for the ECD study is of oligo(arylenethienylene)s, whose general structure is shown in Fig. 1a. In these structures, the substituent introduced on the central arylene core tunes their supramolecular organization depending of the chemical nature of the chiral substituent group, as demonstrated in our previous studies. We studied in detail the chiroptical properties of a series of structurally related (arylenethienylene)s with benzo[1,2-*b*:4,5-*b*′]dithiophene, 9*H*-carbazole and 1,4-phenylene cores bearing the 3,7-dimethyl-1-octyl alkyl chain as chiral element (Fig. 1a);[34–38] this chiral appendage was easily prepared in enantiopure form from a natural terpene (*i.e.*, β-citronellol),[39] and was devoid of functionalities and transfers its molecular asymmetry (*i.e.*, a chiral centre at position 3 of the aliphatic chain) to the entire system (*i.e.*, chirality at supramolecular and mesoscopic scales) exclusively through dispersion forces and steric effects. Another approach involves the use of proteinogenic α-amino acids or monosaccharides as chiral pendant groups; on one hand, the α-amino acid units are able to form multiple and highly directional non-covalent interactions through hydrogen-bonding, and therefore may impact in different ways the chiral supramolecular organization of the oligo(arylenethienylene) backbone; on the other, the monosaccharides units are chiral and polar bulky appendages which may lead to reduced torsional freedom.

In this work, we investigated the (chiro)optical properties of a family of disubstituted phenylene–thiophene oligomers **1–3**, decorated on the phenyl ring by enantiopure α-amino acids or monosaccharide units (Fig. 1b). We selected the *t*BOC-protected L-phenylalanine moiety, linked to the phenylene core through a flexible spacer (a linear six-carbon-atom oxaalkyl chain), in order to favour intermolecular π-stacking and hydrogen bonding interactions. Conversely, we used peracetylated glucose units directly bound to the 1,4-phenylene ring through a β-glucosidic linkage, *i.e.*, without a linear spacer, in order to evaluate the effect of steric hindrance. ECD measurements on chiral conjugated structures **1–3** were performed in both solution aggregation and thin film states to provide unique information about their first level of supramolecular organization, discovering in some cases the co-existence of multiple aggregation pathways which would not have been identified by using UV-Vis absorption spectroscopy alone.

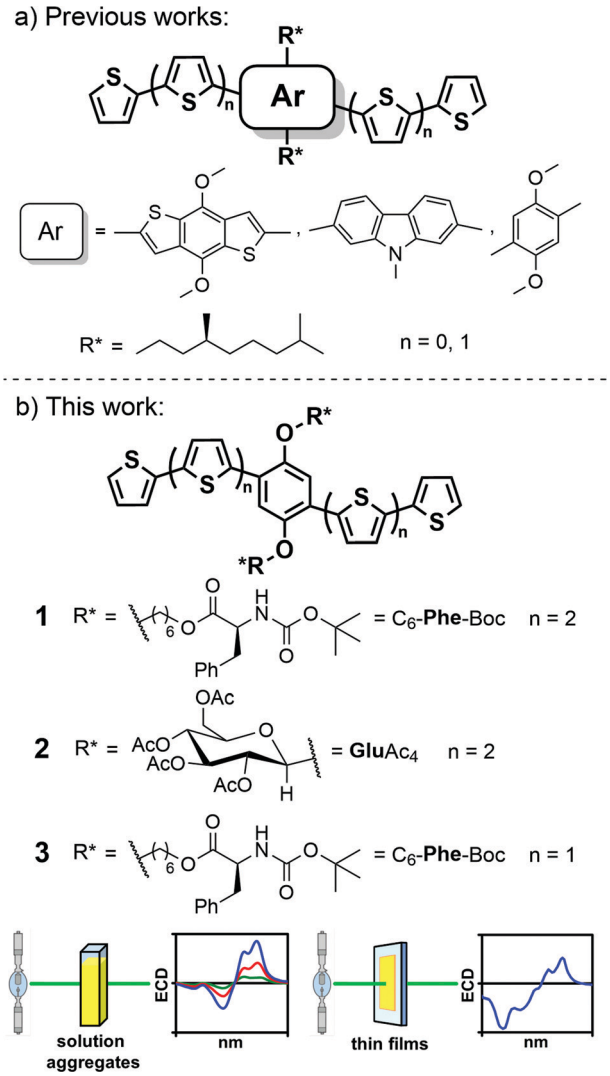

Fig. 1 Scope of the work: three L-phenylalanine- or D-glucose-functionalized phenylene–thiophene oligomers **1–3** have been investigated by electronic circular dichroism (ECD) spectroscopy in both solution aggregation and thin film states, in order to study the impact of chirality on their aggregation modes.

Results and discussion

The three chiral oligo(*p*-phenylenethienylene)s **1–3** were synthesized in good yields according to our previously reported procedure,[40] a versatile synthetic protocol based on the Suzuki–Miyaura cross-coupling reaction.[41,42]

The aggregation modes of the phenylene–thiophene oligomers **1–3** were first studied in solution. In particular, their behaviour in different solvent mixtures, consisting of a good solvent (*i.e.*, chloroform or THF) and a poor solvent or non-solvent (*i.e.*, methanol or water) was investigated. The relevant

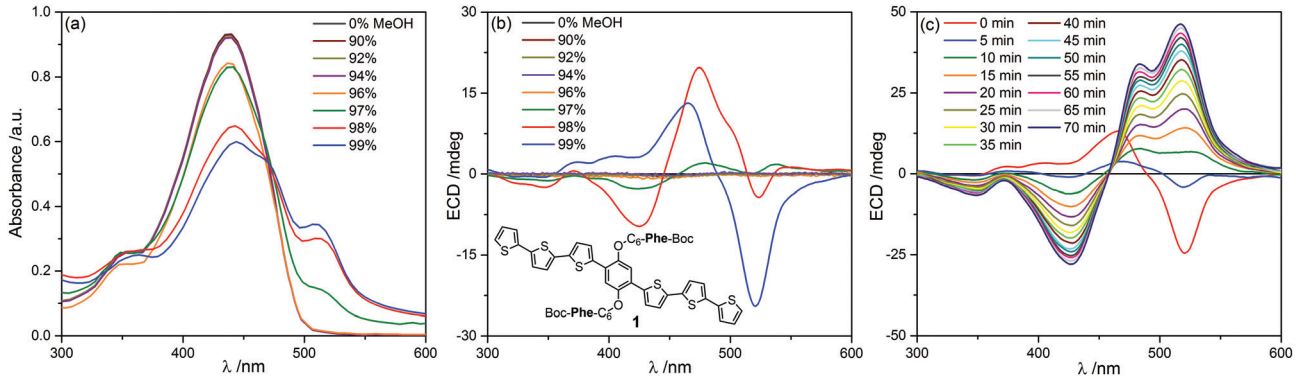

Fig. 2 (Chiro)optical characterization of L-phenylalanine-functionalized phenylene–thiophene oligomer **1** in solution; (a) UV-Vis absorption and (b) ECD spectra in $CHCl_3$/MeOH mixtures with increasing amounts of MeOH; (c) evolution of the ECD spectrum in 99% MeOH as a function of time. Sample concentration: 6×10^{-5} M; cell length: 0.2 cm.

solutions or suspensions were characterized by UV-Vis absorption and ECD spectroscopies. The spectral profiles obtained by the progressive addition of a non-solvent represent the step-by-step picture of the aggregation process. The results obtained by this experimental approach are expected to be in good agreement with the material's solid state behaviour, including thin films.

The (chiro)optical characterization of L-phenylalanine-functionalized oligomer **1** was performed in $CHCl_3/CH_3OH$ mixtures (Fig. 2). As it is soluble in chlorinated solvents, only molecularly dispersed non-aggregated species can be observed in $CHCl_3$ solution. The UV-Vis absorption spectrum in $CHCl_3$ (Fig. 2a, grey line) showed a broad band with the maximum centered at 440 nm, attributable to the $\pi \rightarrow \pi^*$ transition of the *p*-phenylene–thiophene conjugated backbone. The corresponding ECD spectrum (Fig. 2b, grey line) was very weak with dissymmetry factors g_{abs} (defined as $\Delta\varepsilon/\varepsilon$ or $\Delta A/A$) of about 10^{-5}, indicating that the perturbation exerted on the intrinsically achiral π-conjugated chromophore of **1** by individual chiral centres of the two L-phenylalanine moieties is very small in dissolved molecules. The formation of solution supramolecular aggregates can be favoured by the addition of significant amounts of methanol as a poor solvent. In the UV-Vis absorption spectra recorded from a mixed solvent (Fig. 2a), we observed solvatochromism starting from 97% MeOH; the main band was slightly red-shifted and included a shoulder at 481 nm, while a new narrow band (the so-called "aggregation band") appeared at 512 nm, which increased rapidly in intensity by further addition of methanol. The changes in the absorption spectrum offered an unequivocal proof for the occurrence of solution aggregates; on one hand, the aggregation induces an increased planarization of the oligothiophene backbone which causes the slight red-shift of the pristine absorption band;[43–47] on the other hand, the new band at 512 nm is a typical manifestation of self-assembly promoted by π-stacking between the aromatic backbones as well as by ancillary interactions between the side-chains[48,49] (in the current case, hydrogen bonding of L-phenylalanine moieties). However, ECD spectra (Fig. 2b) provided us more insight into the aggregation modes of chiral oligomer **1**. By progressive addition of methanol, significantly different ECD profiles were observed; in 97% MeOH, a weakly structured ECD signal appeared which may be described as a positive exciton couplet, with maximum dissymmetry factor $g_{abs} = 1.3 \times 10^{-4}$ (Fig. 2b, green line); in 99% MeOH, a more pronounced negative exciton couplet was found, which attained maximum $g_{abs} = -2.5 \times 10^{-3}$ (Fig. 2b, blue line), almost 250-fold larger than that of molecularly isolated species in pure chloroform. In both cases, a pronounced long-wavelength tailing appeared as a typical distortion, due to the scattering by suspended particles, confirming the presence of solution aggregates. A further aspect came from the study of the ECD spectrum in 99% MeOH as a function of time (Fig. 2c); we clearly observed a progressive evolution from the above-mentioned negative exciton couplet (t = 0 min) to an asymmetric positive exciton couplet (t = 70 min), having a similar shape (but higher intensity) to the spectrum in 97% MeOH. In order to confirm the genuinity of these ECD results, we have also ruled out the occurrence of any kind of artifact due to linear dichroism (LD) by simultaneously recording the corresponding LD spectra; as expected, in all cases we found negligible signals.

All these results suggested that the chiral oligomer **1** could adopt two concomitant aggregation pathways, leading to different supramolecular structures held together by the π-stacking of conjugated backbones and the hydrogen bonding of α-amino acid moieties in the side chains, with a well-defined helicity between π-conjugated chains packed on the top of each other; a kinetic or metastable aggregation state, associated with the negative ECD couplet and characterized by a left-handed supramolecular helicity, or a thermodynamic aggregation state, responsible for the positive ECD couplet due to a right-handed supramolecular helicity. In this context, the amount of methanol plays an important role in determining which aggregation pathway will be assumed. As the good solvent (*i.e.*, $CHCl_3$) may help in supramolecular rearrangements, by increasing the fraction of the non-solvent (*i.e.*, MeOH) the evolution from the kinetic to thermodynamic aggregation state will be slower. Therefore, in 97% MeOH, chiral oligomer **1** self-assembles

directly into the most thermodynamically stable aggregation state, while in 99% MeOH, it is first trapped into the kinetic state, from which progressively evolves through a simple re-ordering process towards the thermodynamic one within 70 minutes (Fig. 2c). Conversely, the evolution of UV-Vis absorption in 99% MeOH as a function of time (see Fig. S1 in ESI†) showed no changes, confirming that ECD spectroscopy is able to reveal the multiple aggregation pathways of chiral π-conjugated materials, a field of investigation which is limitedly accessible by other spectroscopies.

In order to describe which intermolecular interactions are responsible for the solution aggregates, we also developed a computational model for a hexamer of aggregated chains of the phenylene–thiophene oligomer **1** (Fig. 3), showing π-conjugated backbones arranged into a right-handed supramolecular helicity (*i.e.*, in agreement with the above mentioned thermodynamic aggregation state). The backbones are at a reciprocal distance of 4 Å and present a twist angle $\tau = 15^{\circ}$. The network of hydrogen bonds is represented by dotted green lines. Although the model was obtained with a simplified molecular modelling procedure (see ESI†), it confirmed that hydrogen bonding is largely responsible for the formation of stable supramolecular aggregates, inducing the helical twist between adjacent π-conjugated backbones responsible for the exciton couplet in the ECD spectrum. Moreover, similar to some α-amino acid-functionalized poly(*p*-phenylene ethynylene)s previously reported in the literature,[50] the hydrogen bonding network resembles that of polypeptide parallel β-sheets, with both amide groups of each molecule acting as hydrogen-bond donors for the ester moieties of the adjacent one.

With peracetylated D-glucopiranose units directly bound to the π-conjugated backbone without any linear spacer, chiral phenylene–thiophene **2** is devoid of hydrogen bond donors and is more sterically hindered. These differences with respect to oligomer **1** clearly influenced its optical and chiroptical

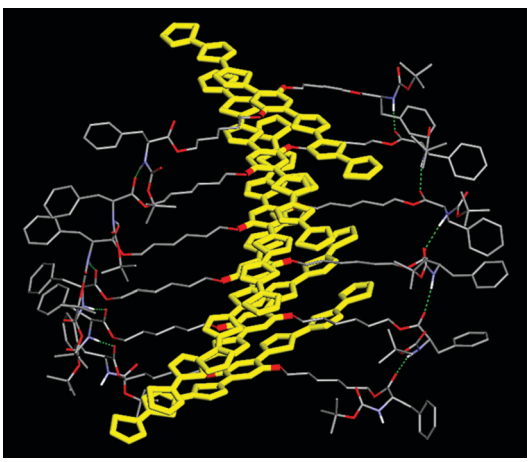

Fig. 3 Computational model for a hexamer of aggregated chains of phenylene–thiophene oligomer **1**, showing the right-handed supramolecular helicity of π-conjugated backbones (in yellow), the relative disposition of the L-phenylalanine-functionalized side chains (in grey), and the hydrogen bond network (dotted green lines).

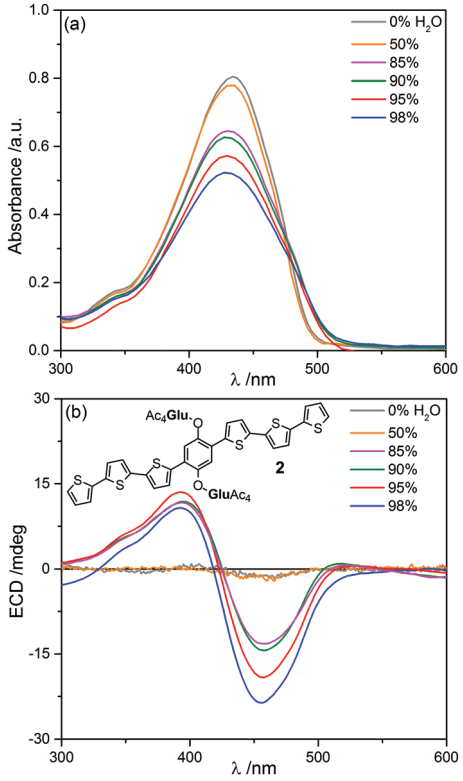

Fig. 4 (Chiro)optical characterization of D-glucose-functionalized phenylene–thiophene oligomer **2** in solution; (a) UV-Vis absorption and (b) ECD spectra in THF/H_2O mixtures with increasing amounts of H_2O. Sample concentration: 6×10^{-5} M; cell length: 0.2 cm.

characteristics. In $CHCl_3/CH_3OH$ mixtures, the absorption spectra of **2** (Fig. S2a in ESI†) showed only negligible differences with that recorded in pure $CHCl_3$ and no evident relationship between the spectral profile and the increasing amount of non-solvent could be found. Likewise, the ECD spectra (Fig. S2b, ESI†) were very weak and with dissymmetry factors g_{abs} always $<10^{-4}$. Such results suggested the absence of supramolecular aggregates in $CHCl_3/CH_3OH$ solvent mixtures; the increased steric hindrance, together with the absence of sites acting as hydrogen bonding donors, makes the self-assembly of π-conjugated backbones of **2** into chiral supramolecular aggregates more difficult with respect to α-amino acid-functionalized oligomer **1**. However, a different behaviour was found by changing the solvent mixture, using THF as the "good" solvent and H_2O as the "poor" solvent (Fig. 4). The UV-Vis absorption spectrum of **2** in pure THF (Fig. 4a, grey line) showed a broad band centered at 435 nm, due to the $\pi \rightarrow \pi^*$ transition of the *p*-phenylene–thiophene backbone. With the addition of considerable amounts of H_2O, we observed the gradual appearance of a small shoulder at 479 nm attributable to the formation of solution aggregates. ECD spectra (Fig. 4b) again provided us more information on the self-assembly behaviour of the chiral oligomer **2**; starting from 85% content in H_2O, the occurrence of a negative exciton couplet was found, with an increasing intensity at higher amounts of non-solvent, attaining the maximum g_{abs} of -1.7×10^{-3} in 98% H_2O (Fig. 4b, blue line).

Moreover, the ECD spectra did not show changes as a function of time.

These findings pointed at the occurrence of a single, thermodynamically stable aggregation mode in oligomer **2**; a supramolecular structure with π-conjugated chains arranged into a right-handed helicity, responsible for the negative ECD couplet. In particular, the steric hindrance of monosaccharide units directly linked to the phenylene moiety increased the distance between adjacent π-conjugated chains, making the exciton coupling less effective with respect to oligomer **1**, and thus justifying the lower values of dissymmetry factor attained ($g_{abs}^{max} = -2.5 \times 10^{-3}$ in 99% MeOH for **1** *vs.* $g_{abs}^{max} = -1.7 \times 10^{-3}$ in 98% H_2O for **2**).

The chiral phenylene–thiophene **3** was successfully used as an active layer in a sensor based on organic thin film transistors (OTFTs) for the discrimination of chiral analytes in the vapour phase.[22] However, here for the first time we report its spectroscopic and chiroptical features. This material structurally differs from **1** for the shorter length of π-conjugated oligothiophene segments (two bithiophene units instead of two terthiophene ones). Interestingly, **3** showed a dramatically different behaviour from **1** in solution aggregation processes. We first investigated its (chiro)optical properties in $CHCl_3$/CH_3OH mixtures (see Fig. S3 in the ESI†). Surprisingly, the absence of supramolecular aggregates was observed, with very weak ECD signals (g_{abs} of about 10^{-5}) regardless of the amount of MeOH added as the non-solvent. This system is less prone to self-assembly than **1** under the same conditions, probably because π–π interactions are weaker due to the shorter length of π-conjugated segments.

By switching to other solvent/non-solvent mixtures, a partially different behaviour was observed in THF/H_2O (Fig. 5). The UV-Vis absorption spectrum of **3** in pure THF (Fig. 5, blue line) showed the main broad band with maximum at 413 nm, associated with the π → π* transition. By increasing the amount of non-solvent, we observed clear solvatochromism starting from 70% H_2O (Fig. 5, red line), with a 10 nm red-shifted main absorption band and the appearance of a shoulder at 457 nm, attesting the occurrence of supramolecular aggregation. The corresponding ECD spectra (see Fig. S4 in ESI†) were very weak, with dissymmetry factors $g_{abs} \sim 10^{-5}$. Such results could be explained by hypothesizing the self-assembly of oligomer **3** chains into ordered achiral supramolecular structures, where the perfect cofacial stacking of π-conjugated chains is preferred compared to a helical twisted one. This result could be influenced by a hydrophobic effect caused by the use of H_2O as a non-solvent. A different possible explanation involves the participation of water in supramolecular aggregation, by the formation of bridge bonds between two adjacent oligomer molecules thanks to hydrogen bonds; this would create less torsion between adjacent π-conjugated chains, favouring an achiral ordered stacking.

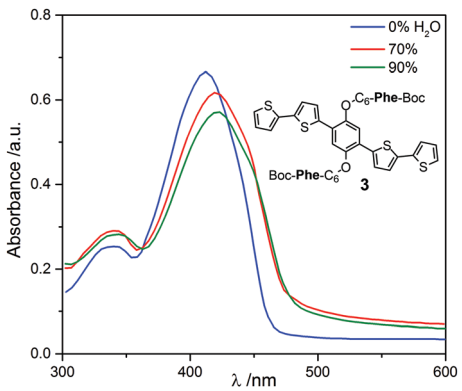

Fig. 5 Optical characterization of L-phenylalanine-functionalized phenylene–thiophene oligomer **3** in solution; UV-Vis absorption spectra in THF/H_2O mixtures with increasing amounts of H_2O. Sample concentration: 6×10^{-5} M; cell length: 0.2 cm.

As mentioned above, the investigation of aggregation modes in solution is often preparatory to their study in the solid state. In particular, the ability to recognize and control different aggregation modes in the case of thin films would be useful for obtaining layers of chiral π-conjugated systems with highly tunable properties for innovative optoelectronic applications.[22] For this reason, the chiro(optical) properties of our chiral oligomers **1–3** were also investigated in thin films.

ECD measurements in thin films require more attention than in isotropic solution, as they may result in more complex spectra due to the interference of macroscopic anisotropies often present in the solid state, *i.e.* linear dichroism (LD) and linear birefringence (LB), which provide a significant contribution to the measured ECD spectrum.[51–53] In particular, the experimental ECD signal of a thin film is the sum of two main contributions: (a) the intrinsic isotropic component of circular dichroism, termed CD_{iso}, which is invariant upon sample orientation and (b) the LDLB, arising from the combined effect of macroscopic anisotropies LD and LB, which inverts the sign by sample flipping.[15] CD_{iso} and LDLB terms can be considered as the chiroptical response of two different hierarchical scales of chirality; CD_{iso} is related to molecular chirality and supramolecular chiral aggregates, while, in certain cases, their further organization into mesoscopic chiral domains can generate a LDLB contribution.[15] Therefore, recognizing CD_{iso} and LDLB in the ECD spectra of thin films can provide useful information on their solid state organization at different hierarchy levels.

We prepared thin films of chiral phenylene–thiophene oligomers **1–3** by drop casting (DC) technique; ~100 μL of a chloroform solution of each compound (concentration: 1.0×10^{-3} M) were deposited on quartz plates, followed by slow evaporation of the solvent in a closed chamber saturated with $CHCl_3$ vapours. All the obtained samples, with a thickness of about 100 nm, appeared macroscopically homogeneous and semi-transparent.

To establish the intrinsic anisotropy of the investigated samples, for each thin film sample the ECD was recorded for both front and back side. In all the cases we found same spectral profiles. Therefore, in the following section, we can safely neglect any contribution due to LDLB and attribute all ECD signals to a pure CD_{iso} arising from the occurrence of plain

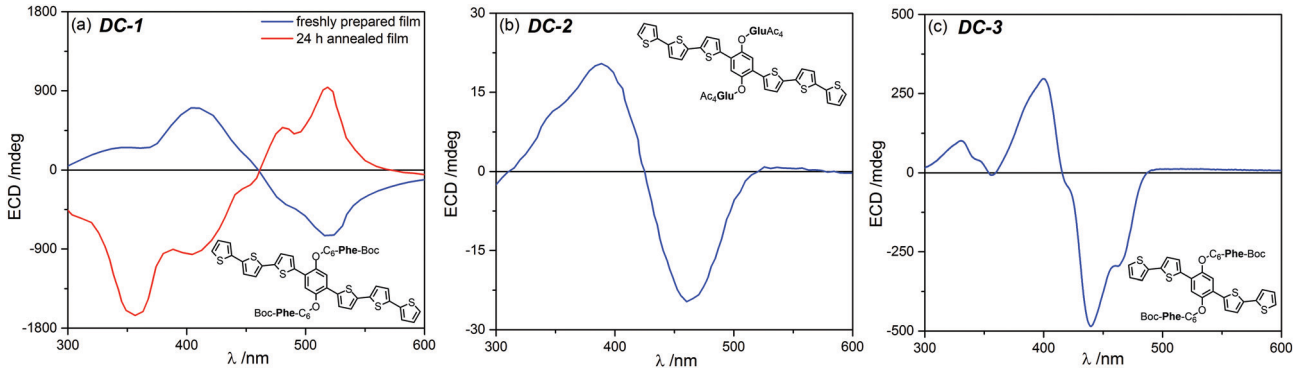

Fig. 6 ECD spectra (normalized with respect to maximum absorbance) recorded for chiral phenylene–thiophene oligomers **1–3** as thin films prepared by drop casting from a $CHCl_3$ solution; (a) drop-casted L-phenylalanine-functionalized oligomer **1** (**DC-1**), as a freshly prepared sample (blue line) and after 24 h of solvent annealing (red line); (b) drop-casted peracetylated D-glucose-functionalized oligomer **2** (**DC-2**); (c) drop-casted L-phenylalanine-functionalized oligomer **3** (**DC-3**).

supramolecular chiral aggregates. We could hypothesize that the steric hindrance of these chiral supramolecular aggregates (responsible for the CD_{iso} contribution) did not allow their further organization into highly anisotropic domains (*i.e.*, characterized by high LD and LB), thus resulting in the absence of any LDLB contribution.

Drop-cast samples of L-phenylalanine-functionalized phenylene–thiophene oligomer **1** (**DC-1**) showed an ECD spectrum with a strong asymmetric negative exciton couplet, with maximum g_{abs} values of -3.9×10^{-2} at 516 nm and $+4.0 \times 10^{-2}$ at 403 nm (Fig. 6a, blue line and Table 1, entry 1). However, a further interesting aspect came from solvent annealing, a typical procedure used to obtain more homogeneous thin films. **DC-1** samples left for 24 h in a chamber saturated with vapours of a "good" solvent (*i.e.*, $CHCl_3$) yielded dramatic changes in the ECD spectrum; a complex, asymmetric positive exciton couplet appeared, with maximum g_{abs} of $+5.4 \times 10^{-2}$ at 519 nm and -9.7×10^{-2} at 357 nm (Fig. 6a, red line and Table 1, entry 2). Interestingly, the ECD spectral shape of freshly prepared and annealed **DC-1** samples resembled that observed for **1** in 99% MeOH at, respectively, $t = 0$ min and $t = 70$ min (Fig. 6a *vs.* 2c). Therefore, the two competing aggregation pathways previously observed for oligomer **1** in solution also occurred in thin films; a kinetic supramolecular order, associated with the negative ECD couplet (Fig. 6a, blue line) and characterized by a left-handed supramolecular helicity, is reached in the short time required for solvent evaporation in the drop-casting process; during the subsequent solvent annealing process, π-conjugated chains rearrange into a thermodynamically stable aggregation state, responsible for the positive ECD couplet (Fig. 6a, red line), due to a right-handed supramolecular helicity. We also recorded the IR spectra of **DC-1** as a freshly prepared sample and after 24 h of solvent annealing (Fig. S6, ESI†); although both provided evidence of hydrogen bonding interactions, thus confirming their role in the supramolecular organization of the oligomer **1**, no significant differences were actually found between them. This is a further confirmation of the importance of ECD spectroscopy in detecting the possible co-existence of multiple aggregation pathways, succeeding where other techniques failed.

Concerning oligomer **2**, the steric hindrance of monosaccharide units exerted a clear effect on its chiroptical properties in thin films. In fact, the ECD spectrum of **DC-2** showed much less intense signals with respect to **DC-1** (almost two orders of magnitude smaller); a negative exciton couplet with dissymmetry factor g_{abs} values of -9.4×10^{-4} at 460 nm and $+8.1 \times 10^{-4}$ at 389 nm (Fig. 6b and Table 1, entry 3), suggesting the occurrence of a supramolecular architecture with a right-handed helicity, although with a less effective exciton coupling of π-conjugated chains with respect to **1**. In this case, we observed no evolution of the chiroptical signals upon solvent annealing, confirming the hypothesis of formation of a single, thermodynamically stable aggregation state.

However, the most interesting chiroptical properties were observed for drop-cast thin films of chiral phenylene–thiophene oligomer **3** (**DC-3**), since it did not show any significant ECD signal in a variety of solvent mixtures. The ECD spectrum of **DC-3** showed a complex and strong, asymmetric negative couplet, which attained a maximum dissymmetry factor g_{abs} value of -1.7×10^{-2} at 440 nm and $+1.2 \times 10^{-2}$ at 400 nm. Such results could be explained by hypothesizing the occurrence of a chiral supramolecular architecture with a strong left-handed helical twist between adjacent π-conjugated backbones. **DC-3** samples retained the same ECD spectrum after solvent

Table 1 Chiroptical properties of chiral phenylene–thiophene oligomers **1–3** as thin films prepared by drop casting from a $CHCl_3$ solution and dissymmetry factor g_{abs} values recorded at two representative wavelengths

Entry	Thin film sample	λ (nm)	g_{abs}
1	**DC-1** (freshly prepared)	403	$+4.0 \times 10^{-2}$
		516	-3.9×10^{-2}
2	**DC-1** (24 h annealed)	357	-9.7×10^{-2}
		519	$+5.4 \times 10^{-2}$
3	**DC-2**	389	$+8.1 \times 10^{-4}$
		460	-9.4×10^{-4}
4	**DC-3**	400	$+1.2 \times 10^{-2}$
		440	-1.7×10^{-2}

annealing (24 h under $CHCl_3$ vapours), suggesting that the observed aggregation mode corresponded to an energetically stable situation. Moreover, since chiral oligomer **3** is the only compound whose chiroptical properties in solution and films were not similar, we ruled out the occurrence of any kind of artifact by repeating the same measurements on thin films of the opposite enantiomer of **3**, *i.e.*, D-phenylalanine-decorated phenylene–thiophene oligomer (*ent*-**3**); a specular ECD spectrum with a positive couplet was obtained (Fig. S7, ESI†), confirming the total reproducibility of our results. However, this difference between solution and thin films ECD properties is actually not surprising; if oligomer **3** is less prone to self-assembly in solution because π–π interactions are less effective due to the shorter π-conjugated length, then with the removal of $CHCl_3$ by slow evaporation in drop-cast thin films, an efficient π-packing into chiral supramolecular architectures is still possible.

It is worth emphasizing that phenylene–thiophene oligomers **1** and **3** exhibited intense ECD signals in thin films, with g_{abs} values in the order of 10^{-2} (and up to about 0.1 in the case of annealed **DC-1** sample). This ability of displaying high (or very high) discrimination in the absorption of CP light would be highly desirable in thin films of chiral organic semiconductors, as it could open the way to their application as active layers in innovative optoelectronic devices, for example CP light-detecting organic field-effect transistors.[54,55]

Conclusions

In conclusion, we studied the (chiro)optical properties of three chiral phenylene–thiophene oligomers functionalized with enantiopure L-phenylalanine or D-glucopiranose moieties, in both solution aggregation and thin film states. We investigated the impact of chirality on their aggregation modes, evaluating the effect of both intermolecular hydrogen bonding and dispersion forces, as well as the role played by steric hindrance and π-conjugated length in promoting different supramolecular architectures. We demonstrated that ECD provides unique and valuable information about the first level of supramolecular organization, discovering in some cases the co-existence of multiple aggregation pathways which would not have been identified by using only UV-Vis absorption spectroscopy. The ability to recognize and finely control these different aggregation modes, enabled by our study, is very useful for obtaining layers of chiral organic semiconductors with highly tunable properties (in particular with strong dissymmetry factor g_{abs} values) especially in the case of thin films for optoelectronic applications.

Conflicts of interest

There are no conflicts to declare.

Acknowledgements

The authors are indebted to Prof. Gennaro Pescitelli for his help in the computational model calculations and to Prof. Lorenzo Di Bari for the fruitful discussions. Q2

Notes and references

1 O. Ostroverkhova, *Chem. Rev.*, 2016, **116**, 13279–13412.
2 P. Friederich, A. Fediai, S. Kaiser, M. Konrad, N. Jung and W. Wenzel, *Adv. Mater.*, 2019, **31**, 1808256.
3 U. Mitschke and P. Bäuerle, *J. Mater. Chem.*, 2000, **10**, 1471–1507.
4 G. M. Farinola and R. Ragni, *Chem. Soc. Rev.*, 2011, **40**, 3467–3482.
5 A. Facchetti, *Chem. Mater.*, 2011, **23**, 733–758.
6 C. Wang, H. Dong, W. Hu, Y. Liu and D. Zhu, *Chem. Rev.*, 2012, **112**, 2208–2267.
7 M. A. Rahman, P. Kumar, D.-S. Park and Y.-B. Shim, *Sensors*, 2008, **8**, 118–141.
8 J. Cornil, D. Beljonne, J.-P. Calbert and J.-L. Brédas, *Adv. Mater.*, 2001, **13**, 1053–1067.
9 F. J. M. Hoeben, P. Jonkheijm, E. W. Meijer and A. P. H. J. Schenning, *Chem. Rev.*, 2005, **105**, 1491–1546.
10 T. L. Andrew and T. M. Swager, *J. Polym. Sci., Part B: Polym. Phys.*, 2011, **49**, 476–498.
11 A. Salleo, R. J. Kline, D. M. DeLongchamp and M. L. Chabinyc, *Adv. Mater.*, 2010, **22**, 3812–3838.
12 J. Rivnay, S. C. B. Mannsfeld, C. E. Miller, A. Salleo and M. F. Toney, *Chem. Rev.*, 2012, **112**, 5488–5519.
13 P. A. Korevaar, T. F. A. de Greef and E. W. Meijer, *Chem. Mater.*, 2014, **26**, 576–586.
14 Y. Dorca, E. E. Greciano, J. S. Valera, R. Gómez and L. Sánchez, *Chem. – Eur. J.*, 2019, **25**, 5848–5864.
15 G. Albano, G. Pescitelli and L. Di Bari, *Chem. Rev.*, 2020, **120**, 10145–10243.
16 M. Verswyvel and G. Koeckelberghs, *Polym. Chem.*, 2012, **3**, 3203–3216.
17 Y. Yang, Y. Zhang and Z. Wei, *Adv. Mater.*, 2013, **25**, 6039–6049.
18 M. Liu, L. Zhang and T. Wang, *Chem. Rev.*, 2015, **115**, 7304–7397.
19 C. Resta, S. Di Pietro, M. Majerić Elenkov, Z. Hameršak, G. Pescitelli and L. Di Bari, *Macromolecules*, 2014, **47**, 4847–4850.
20 C. C. Lee, C. Grenier, E. W. Meijer and A. P. H. J. Schenning, *Chem. Soc. Rev.*, 2009, **38**, 671–683.
21 L. A. P. Kane-Maguire and G. G. Wallace, *Chem. Soc. Rev.*, 2010, **39**, 2545–2576.
22 L. Torsi, G. M. Farinola, F. Marinelli, M. C. Tanese, O. H. Omar, L. Valli, F. Babudri, F. Palmisano, P. G. Zambonin and F. Naso, *Nat. Mater.*, 2008, **7**, 412–417.
23 C. Train, M. Gruselle and M. Verdaguer, *Chem. Soc. Rev.*, 2011, **40**, 3297–3312.
24 P. C. Mondal, C. Fontanesi, D. H. Waldeck and R. Naaman, *Acc. Chem. Res.*, 2016, **49**, 2560–2568.

25 J. G. Ibanez, M. E. Rincón, S. Gutierrez-Granados, M. H. Chahma, O. A. Jaramillo-Quintero and B. A. Frontana-Uribe, *Chem. Rev.*, 2018, **118**, 4731–4816.

26 J. R. Brandt, F. Salerno and M. J. Fuchter, *Nat. Rev. Chem.*, 2017, **1**, 0045.

27 V. Palermo and P. Samorì, *Angew. Chem., Int. Ed.*, 2007, **46**, 4428–4432.

28 N. Berova, L. D. Bari and G. Pescitelli, *Chem. Soc. Rev.*, 2007, **36**, 914–931.

29 G. Pescitelli, L. Di Bari and N. Berova, *Chem. Soc. Rev.*, 2011, **40**, 4603–4625.

30 G. Pescitelli, L. Di Bari and N. Berova, *Chem. Soc. Rev.*, 2014, **43**, 5211–5233.

31 M. Górecki, M. A. M. Capozzi, G. Albano, C. Cardellicchio, L. Di Bari and G. Pescitelli, *Chirality*, 2018, **30**, 29–42.

32 R. D. McCullough, *Adv. Mater.*, 1998, **10**, 93–116.

33 I. F. Perepichka, D. F. Perepichka, H. Meng and F. Wudl, *Adv. Mater.*, 2005, **17**, 2281–2305.

34 G. Albano, M. Lissia, G. Pescitelli, L. A. Aronica and L. Di Bari, *Mater. Chem. Front.*, 2017, **1**, 2047–2056.

35 G. Albano, F. Salerno, L. Portus, W. Porzio, L. A. Aronica and L. Di Bari, *ChemNanoMat*, 2018, **4**, 1059–1070.

36 G. Albano, M. Górecki, G. Pescitelli, L. Di Bari, T. Jávorfi, R. Hussain and G. Siligardi, *New J. Chem.*, 2019, **43**, 14584–14593.

37 G. Albano, L. A. Aronica, A. Minotto, F. Cacialli and L. Di Bari, *Chem. – Eur. J.*, 2020, **26**, 16622–16627.

38 F. Zinna, G. Albano, A. Taddeucci, T. Colli, L. A. Aronica, G. Pescitelli and L. Di Bari, *Adv. Mater.*, 2020, **32**, 2002575.

39 G. Albano, T. Colli, T. Biver, L. A. Aronica and A. Pucci, *Dyes Pigm.*, 2020, **178**, 108368.

40 O. Hassan Omar, F. Babudri, G. M. Farinola, F. Naso, A. Operamolla and A. Pedone, *Tetrahedron*, 2011, **67**, 486–494.

41 A. Operamolla, S. Colella, R. Musio, A. Loiudice, O. Hassan Omar, G. Melcarne, M. Mazzeo, G. Gigli, G. M. Farinola and F. Babudri, *Sol. Energy Mater. Sol. Cells*, 2011, **95**, 3490–3503.

42 A. Ruiz-Carretero, Y. Atoini, T. Han, A. Operamolla, S. Ippolito, C. Valentini, S. Carrara, S. Sinn, E. A. Prasetyanto, T. Heiser, P. Samorì, G. Farinola and L. De Cola, *J. Mater. Chem. A*, 2019, **7**, 16777–16784.

43 D. Iarossi, A. Mucci, F. Parenti, L. Schenetti, R. Seeber, C. Zanardi, A. Forni and M. Tonelli, *Chem. – Eur. J.*, 2001, **7**, 676–685.

44 F. Brustolin, F. Goldoni, E. W. Meijer and N. A. J. M. Sommerdijk, *Macromolecules*, 2002, **35**, 1054–1059.

45 H. Goto, Y. Okamoto and E. Yashima, *Macromolecules*, 2002, **35**, 4590–4601.

46 A. Mucci, F. Parenti, R. Cagnoli, R. Benassi, A. Passalacqua, L. Preti and L. Schenetti, *Macromolecules*, 2006, **39**, 8293–8302.

47 G. Albano, T. Colli, L. Nucci, R. Charaf, T. Biver, A. Pucci and L. A. Aronica, *Dyes Pigm.*, 2020, **174**, 108100.

48 F. Babudri, D. Colangiuli, L. Di Bari, G. M. Farinola, O. Hassan Omar, F. Naso and G. Pescitelli, *Macromolecules*, 2006, **39**, 5206–5212.

49 G. Pescitelli, O. Hassan Omar, A. Operamolla, G. M. Farinola and L. Di Bari, *Macromolecules*, 2012, **45**, 9626–9630.

50 C. Resta, G. Pescitelli and L. Di Bari, *Macromolecules*, 2014, **47**, 7052–7059.

51 Y. Shindo and M. Nakagawa, *Rev. Sci. Instrum.*, 1985, **56**, 32–39.

52 Y. Shindo, M. Nakagawa and Y. Ohmi, *Appl. Spectrosc.*, 1985, **39**, 860–868.

53 R. Kuroda, T. Harada and Y. Shindo, *Rev. Sci. Instrum.*, 2001, **72**, 3802–3810.

54 Y. Yang, R. C. da Costa, M. J. Fuchter and A. J. Campbell, *Nat. Photonics*, 2013, **7**, 634–638.

55 L. Zhang, I. Song, J. Ahn, M. Han, M. Linares, M. Surin, H.-J. Zhang, J. H. Oh and J. Lin, *Nat. Commun.*, 2021, **12**, 142.